© 2018. Published by The Company of Biologists Ltd | Development (2018) 145, dev158162. doi:10.1242/dev.158162

RESEARCH REPORT

Runx1 is sufficient for blood cell formation from non-hemogenic endothelial cells *in vivo* only during early embryogenesis

Amanda D. Yzaguirre[1], Elizabeth D. Howell[1], Yan Li[1], Zijing Liu[2] and Nancy A. Speck[1,*]

ABSTRACT

Hematopoietic cells differentiate during embryogenesis from a population of endothelial cells called hemogenic endothelium (HE) in a process called the endothelial-to-hematopoietic transition (EHT). The transcription factor Runx1 is required for EHT, but for how long and which endothelial cells are competent to respond to Runx1 are not known. Here, we show that the ability of Runx1 to induce EHT in non-hemogenic endothelial cells depends on the anatomical location of the cell and the developmental age of the conceptus. Ectopic expression of Runx1 in non-hemogenic endothelial cells between embryonic day (E) 7.5 and E8.5 promoted the formation of erythro-myeloid progenitors (EMPs) specifically in the yolk sac, the dorsal aorta and the heart. The increase in EMPs was accompanied by a higher frequency of HE cells able to differentiate into EMPs *in vitro*. Expression of Runx1 just 1 day later (E8.5-E9.5) failed to induce the ectopic formation of EMPs. Therefore, endothelial cells, located in specific sites in the conceptus, have a short developmental window of competency during which they can respond to Runx1 and differentiate into blood cells.

KEY WORDS: Hematopoiesis, Runx1, Hemogenic endothelium, Embryo

INTRODUCTION

Hematopoietic stem and progenitor cells (HSPCs) arise from a subset of endothelial cells called hemogenic endothelium (HE). During gastrulation, Flk1^{+} mesodermal cells migrate from the primitive streak into the yolk sac and embryo proper, where they downregulate mesodermal markers and upregulate endothelial-specific markers coalescing to form a primitive vascular plexus (Coultas et al., 2005; Huber et al., 2004; Sorensen et al., 2009; Walls et al., 2008). The primitive vascular plexus then undergoes extensive remodeling to give rise to a functional cardiovascular system (Coultas et al., 2005; Walls et al., 2008). As the cardiovascular system continues to develop and mature, the endothelial cells acquire one of at least four identities: arterial, venous, lymphatic or hemogenic. HE is located within the large arteries of the embryo, the endocardium of the heart, the chorionic vasculature of the placenta, and the arterial and venous plexus of the yolk sac (Frame et al., 2015; Nakano et al., 2013; Rhodes et al., 2008; Yzaguirre and Speck, 2016). Acquisition of hemogenic identity is regulated in part by the transcription factor Runx1 (Tober et al., 2016). When Runx1 is knocked out in the germ line, or ablated via endothelial-specific Cre-recombinase-mediated excision, the HE-to-HSPC transition is abrogated (Chen et al., 2009; North et al., 1999; Yokomizo et al., 2001).

Ectopic lentiviral expression of Runx1 in non-hemogenic endothelial cell progenitors from embryonic day (E) 8.5 mouse embryos could efficiently re-specify them as hemogenic (Eliades et al., 2016). On the other hand, the respecification of human adult endothelium by ectopic expression of Runx1 was relatively inefficient (Sandler et al., 2014). Although these two experiments were performed in different laboratories, the data suggest that not all non-hemogenic endothelial cells are equally competent to be specified as hemogenic by Runx1.

Here, we show that endothelial cells rapidly lose their competence to respond to Runx1 and differentiate into HSPCs within the intact conceptus. The endothelial cells capable of producing HSPCs are located in specific anatomical sites, in close proximity to normal blood-producing sites. Finally, we show that endothelial cells in the embryo proper are incapable of differentiating into HSPCs *in vivo*, but can efficiently do so *in vitro*, indicating that they can be specified by Runx1 as hemogenic, but are located in a non-permissive environment for blood cell formation in the embryo.

RESULTS AND DISCUSSION

We determined whether non-hemogenic endothelium in the conceptus could be specified as HE and differentiate into HSPCs *in vivo* following the ectopic expression of Runx1. To limit ectopic expression of Runx1 to the endothelium, we generated conceptuses with a conditionally activated *Runx1* cDNA expressed from the *Rosa26* locus [*Gt(ROSA)26*$^{tm1(RUNX1)Ma}$, referred to throughout as cR1, for conditional Runx1] (Qi et al., 2017), and an endothelial-specific tamoxifen-inducible Cre driven from the vascular endothelial cadherin (*Cdh5*) regulatory sequences [Tg(Cdh5-cre/ERT2)1Rha, referred to as Cre] (Sorensen et al., 2009). Injection of tamoxifen into pregnant mice results in the deletion of a floxed translational stop cassette preceding the Runx1-coding sequences in endothelial cells, and pan-endothelial cell expression of Runx1. Conceptuses containing one cR1 allele are referred to as cR1/+, and those containing two cR1 alleles as cR1/cR1. Intraperitoneal tamoxifen was administered to pregnant dams in all experiments.

HE cells are specified in the mouse between E7.5 and E10.5, and undergo an EHT to become a HSPC between E8.0 and E11.5. To determine whether Runx1 is sufficient to specify non-hemogenic endothelial cells as HE cells *in vivo*, we initiated ectopic endothelial cell expression of Runx1 at E7.5, E8.5 or E9.5, and collected conceptuses for analysis at E10.5, during the peak of endogenous EHT (Fig. 1A). When ectopic Runx1 expression was initiated at E7.5 by injection of 1 mg of tamoxifen into pregnant mice, the conceptuses died by E10.5 from cardiovascular defects (data not

[1]Abramson Family Cancer Research Institute, Department of Cell and Developmental Biology, Institute for Regenerative Medicine, Perelman School of Medicine at the University of Pennsylvania, Philadelphia, PA 19104, USA. [2]Beijing Institute of Biotechnology, Beijing 100850, People's Republic of China.

*Author for correspondence (nancyas@exchange.upenn.edu)

N.A.S., 0000-0002-1893-582X

Received 14 August 2017; Accepted 2 January 2018

Development (2018) 145, dev158162. doi:10.1242/dev.158162

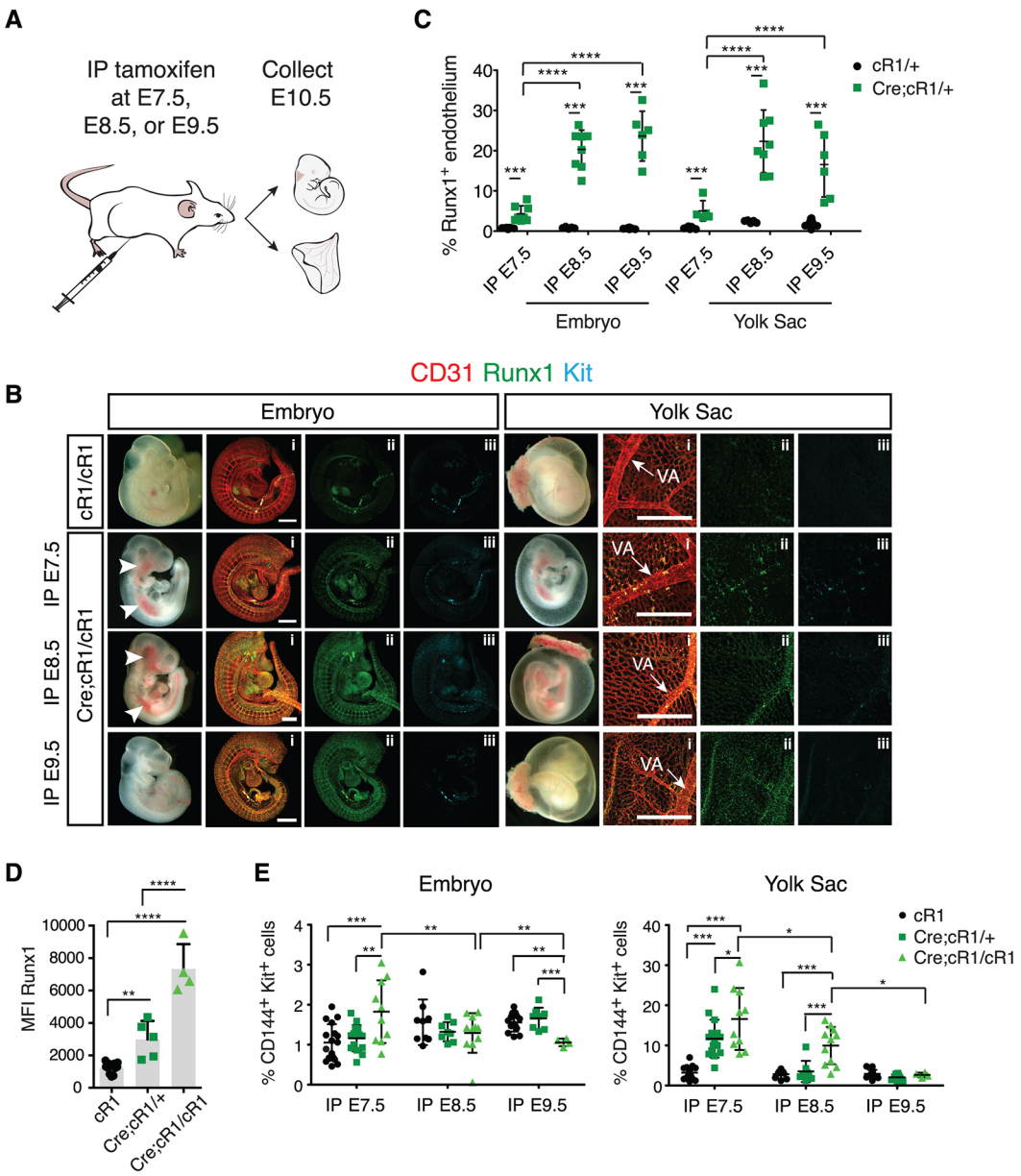

Fig. 1. Conditional endothelial-specific expression of Runx1 initiated before E9.5 increases phenotypic HSPCs in the yolk sac and embryo. (A) Experimental outline for the initiation of ectopic endothelial-specific expression of Runx1 *in utero* at embryonic day (E) 7.5, E8.5 or E9.5 by the intraperitoneal (IP) injection of tamoxifen into pregnant mice and the subsequent collection of embryos and yolk sacs for analysis at E10.5. (B) Gross images and confocal *z*-projections of cR1/cR1 and Cre;cR1/cR1 embryos and yolk sacs. Samples were immunostained for CD31 (i), Runx1 (i,ii) and Kit (i,iii). Arrowheads in the gross images indicate sites of hemorrhaging; arrows in yolk sac images indicate the vitelline artery (VA). Scale bars: 500 µm. (C) Percentage of endothelial cells ($CD144^+$ $CD31^+$ $CD41^-$ $CD45^-$ $Ter119^-$) expressing Runx1 in the embryo and yolk sac of E10.5 cR1/+ and Cre;cR1/+ littermates after the initiation of Runx1 expression at E7.5, E8.5 or E9.5 (mean±s.d.). Unpaired two-tailed Student's *t*-test was used for comparison of paired littermates (horizontal lines, two litters per time point). Differences between all samples were determined using one-way ANOVA and Tukey's multiple comparison test (brackets). ***$P\leq0.001$; ****$P\leq0.0001$. (D) Median fluorescence intensity (MFI) of intracellular Runx1 in $CD144^+CD31^+$ cells. cR1=cR/+ and cR1/cR1 combined; all embryos were from dams injected with tamoxifen at E9.5 and harvested at E10.5. Differences between all samples were determined by one-way ANOVA and Tukey's multiple comparison test (brackets). **$P\leq0.01$, ****$P\leq0.0001$. Data from three litters in three separate experiments. (E) Percentage of $CD144^+$ Kit^+ cells in the embryo and yolk sac of E10.5 controls (cR1=cR/+ and cR1/cR1 combined), Cre;cR1/+ and Cre;cR1/cR1 conceptuses after initiation of ectopic Runx1 expression at E7.5, E8.5 or E9.5. Data are from four to six litters per time point (mean±s.d.). One-way ANOVA and Tukey's multiple comparison tests were used. ***$P\leq0.001$, **$P\leq0.01$, *$P\leq0.05$.

shown). To prevent lethality, we decreased the percentage of endothelial cells ectopically expressing Runx1 by reducing the dose of tamoxifen to 0.5 mg, which caused hemorrhaging in the head and dorsal region of the embryo, which is indicative of vascular defects (Fig. 1B, arrowheads), but nevertheless yielded viable E10.5 conceptuses. Injection of 1 mg tamoxifen and initiation of ectopic Runx1 expression at E8.5 or E9.5 also caused hemorrhaging, but in both cases E10.5 conceptuses were viable (Fig. 1B, arrowheads). Therefore, to achieve both viability and the highest percentages of endothelium ectopically expressing Runx1 at each time point, we used 0.5 mg of tamoxifen to initiate ectopic Runx1 expression at E7.5 and 1 mg at E8.5 and E9.5. Only viable embryos with beating

Development (2018) 145, dev158162. doi:10.1242/dev.158162

hearts and comparable numbers of somite pairs were analyzed throughout this study.

To confirm that Runx1 was ectopically expressed in endothelium, we determined the percentage of Runx1$^+$ endothelial cells (CD45$^-$ CD41$^-$ Ter119$^-$ CD31$^+$ CD144$^+$) in E10.5 conceptuses by flow cytometry (Fig. 1C, Fig. S1A). Fewer than 1% of endothelial cells in the embryo and ∼2% in the yolk sac are Runx1$^+$ in E10.5 control conceptuses (cR1/+) (Fig. 1C). The percentage of Runx1$^+$ endothelial cells was significantly higher in E10.5 embryos and yolk sacs containing Cre and one conditional *Runx1 Rosa26* allele (Cre;cR1/+) following injection of pregnant dams with tamoxifen at all three time points (Fig. 1C). The percentages of Runx1$^+$ endothelial cells were lower at E10.5 when Runx1 expression was initiated at E7.5 compared with induction at E8.5 and E9.5, most likely due to the lower dose of tamoxifen used at E7.5 (Fig. 1C). Confocal *z*-projections confirmed that Runx1 was ectopically expressed throughout the vasculature of E10.5 embryos and yolk sacs after tamoxifen injection at all three times points (Fig. 1Bi and ii). Endothelial cells in embryos with two conditional *Runx1 Rosa26* alleles (Cre;cR1/cR1) contained ∼2.5-fold more Runx1 than endothelial cells from Cre;cR1/+ embryos, as reflected by the median fluorescence intensity of intracellular Runx1 (Fig. 1D).

We analyzed E10.5 embryos and yolk sacs for the presence of CD31$^+$Runx1$^+$Kit$^+$ hematopoietic cluster cells, a morphological indicator of HSPC formation, by confocal microscopy. Ectopic expression of Runx1 increased CD31$^+$ Runx1$^+$ Kit$^+$ cells in the vascular plexus and vitelline artery in yolk sacs of Cre;cR1/cR1 conceptuses when Runx1 was activated at E7.5, to a lesser extent when induced at E8.5, but had no effect when induced at E9.5 (Fig. 1B). We confirmed and quantified these results by flow cytometry, which demonstrated significant increases in the percentages of CD144$^+$Kit$^+$ cells in the yolk sacs of Cre;cR1/cR1 conceptuses at E7.5 and E8.5, but not at E9.5 (Fig. 1E). To provide additional evidence that the cells were hematopoietic in nature, we analyzed them for expression of the hematopoietic markers CD41 and CD45, and found the majority of Kit$^+$ cells in the yolk sac were positive for one or both markers (Fig. S1B,C).

The competency of endothelial cells to produce HSPCs in response to Runx1 decreased rapidly with developmental age. This was evidenced both by the reduced percentages of CD144$^+$Kit$^+$ cells in Cre;cR1/cR1 yolk sacs and embryos following Runx1 induction at E8.5 compared with induction at E7.5, and at E9.5 compared with E8.5 (Fig. 1E). In addition, there was a stricter dose requirement for Runx1 after E7.5, as induction of Runx1 expression at E7.5 increased the percentage of CD144$^+$Kit$^+$ cells in both Cre;cR1/+ and Cre;cR1/cR1 yolk sacs, but at E8.5 only Cre;cR1/cR1 yolk sacs contained a higher percentage of CD144$^+$Kit$^+$ cells (Fig. 1E). Therefore, at E7.5, endothelial cells in the yolk sac responded more robustly to Runx1 than they did 1 or 2 days later, and E7.5 endothelial cells required lower levels of Runx1 to produce phenotypic HSPCs compared with E8.5 endothelial cells. The loss of competence of endothelial cells to be specified as hemogenic by Runx1 with age is even more pronounced when one considers that the percentage of Runx1$^+$ endothelial cells is significantly lower in E7.5 conceptuses than at the later time points (Fig. 1C).

Endothelial cells in the embryo proper were less competent than those in the yolk sac to respond to Runx1 and produce phenotypic HSPCs *in vivo*, as only injection of tamoxifen at E7.5 increased the percentage of CD144$^+$ Kit$^+$ cells, and this occurred only in embryos containing Cre and two *Rosa26 Runx1* alleles (Cre;cR1/cR1) (Fig. 1E). Activation of Runx1 at E9.5 decreased the percentage of CD144$^+$ Kit$^+$ cells in Cre;cR1/cR1 embryos at E10.5, indicating that high levels of Runx1 between E9.5 and E10.5 in endogenous embryonic hemogenic endothelial cells represses the formation, proliferation or viability of phenotypic HSPCs (Fig. 1E).

We examined E10.5 embryos in which Runx1 expression was induced at E7.5 by confocal microscopy to locate ectopic sites of HSPC formation. We identified two sites, the dorsal aorta and the heart, both of which are close to sites of endogenous hemogenic endothelium. Typically, the majority of hematopoietic cluster cells in the dorsal aorta form on its ventral aspect (Taoudi and Medvinsky, 2007; Yokomizo and Dzierzak, 2010). There was no increase in Kit$^+$ CD31$^+$ Runx1$^+$ cells in the ventral aspect of the dorsal aortas of Cre;cR1/+ and Cre;cR1/cR1 embryos compared with control embryos, indicating that ectopic expression of Runx1 did not enhance HSPC formation from endogenous hemogenic endothelium (Fig. 2A,B). There were, however, more Kit$^+$ CD31$^+$ Runx1$^+$ hematopoietic cluster cells in the dorsal aspect of the dorsal aorta (Fig. 2A,B). We also observed ectopic angiogenic sprouts from Cre;cR1/+ and Cre;cR1/cR1 dorsal aortas that were often associated with phenotypic HSPCs (Fig. S2 and Movies 1, 2).

To determine whether the HSPCs in the dorsal aspect of the dorsal aorta developed from dorsal endothelial cells, and were not due to an expansion or migration of endogenous hemogenic endothelial cells, we induced endothelial cell expression of Runx1 in conceptuses homozygous for a non-functional *Runx1* allele (*Runx1*$^{-/-}$) (Wang et al., 1996). Runx1-deficient conceptuses lack Kit$^+$ hematopoietic cluster cells, thus any Kit$^+$ CD31$^+$ Runx1$^+$ cells in the conceptus would be derived from endothelial cells ectopically expressing Runx1 from the *Rosa26* locus. As expected, there were no Kit$^+$ CD31$^+$ Runx1$^+$ cells in the dorsal aorta of cR1/cR1;*Runx1*$^{-/-}$ embryos (Fig. S3A). Induction of Runx1 expression in Cre;cR1/cR1;*Runx1*$^{-/-}$ embryos resulted in Kit$^+$ CD31$^+$ Runx1$^+$ cells throughout the dorsal aorta, in both its ventral and dorsal aspect. Therefore, Kit$^+$ cells in the dorsal aspect of the dorsal aorta are derived from endothelial cells ectopically expressing Runx1.

The heart is a site of HSPC formation but, unlike the dorsal aorta, the heart generates only transient erythro-myeloid progenitors (EMPs) (Nakano et al., 2013). We found that Cre;cR1/+ and Cre;cR1/cR1 hearts had more Kit$^+$ CD31$^+$ Runx1$^+$ cells when compared with littermate controls (Fig. 2C, arrowheads). As observed in the dorsal aorta, the Kit$^+$ CD31$^+$ Runx1$^+$ cells were also induced in the absence of endogenous Runx1 (Fig. S3C). Ectopic angiogenic sprouts were observed near the atrioventricular canal in 83% of Cre;cR1/+ and Cre;cR1/cR1 hearts (Fig. 2C, arrows). Interestingly, most of the endothelial cells within the angiogenic sprouts did not ectopically express Runx1, suggesting that the sprouts are a secondary effect of ectopic Runx1 expression. Hearts from Cre;cR1/+ and Cre;cR1/cR1 embryos in which Runx1 was induced at E7.5 also contained significantly more EMPs than littermate controls, as measured in colony-forming assays, indicating that ectopic expression of Runx1 in cardiac endothelium increased both phenotypic and functional HSPCs (Fig. 2D).

Ectopic expression of Runx1 in the endothelium at E7.5 increased the number of EMPs in the yolk sac (Fig. 3A,B), paralleling the increase in phenotypic HSPCs (Fig. 1E). There was, however, no increase in progenitors with lymphoid potential, which were enumerated by limiting dilution of purified Kit$^+$ cells on OP9 and OP9-DL1 stromal cells, which promote the differentiation of B and T cells, respectively (Schmitt and Zúñiga-Pflücker, 2006) (Fig. 3C-E). Therefore, endothelial cells ectopically expressing Runx1 yielded HSPCs with erythro-myeloid, and not lymphoid, potential in the yolk sac following induction at E7.5, but not at later time points.

Development (2018) 145, dev158162. doi:10.1242/dev.158162

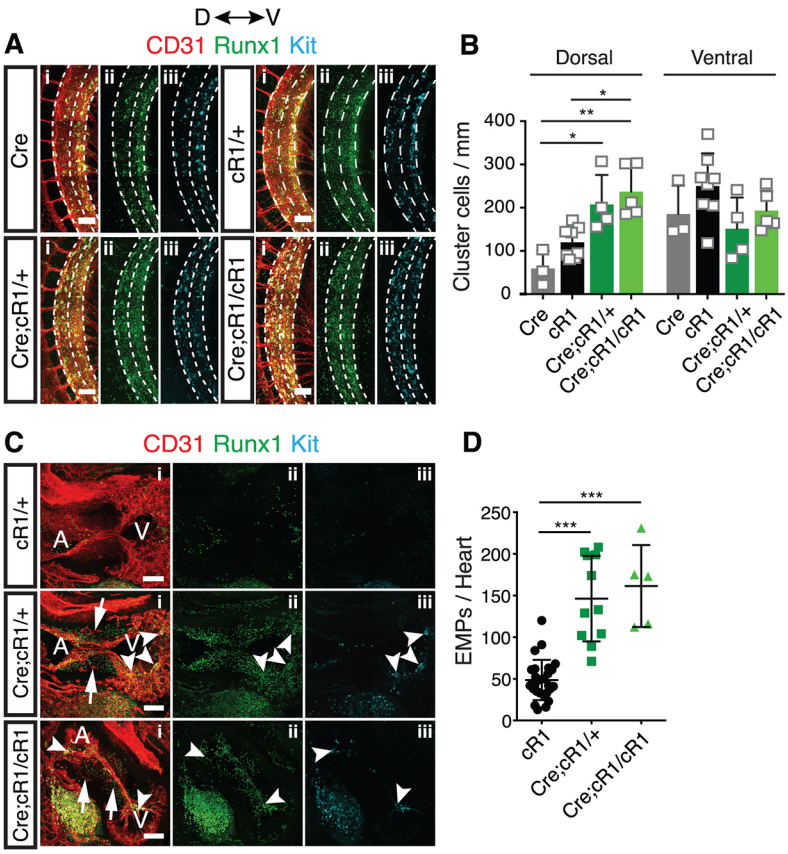

Fig. 2. Conditional endothelial-specific expression of Runx1 initiated at E7.5 increases phenotypic HSPCs in the heart and dorsal aspect of the dorsal aorta (DA). (A) Confocal *z*-projections of DAs with z-intervals of 2 µm from E10.5 embryos immunostained for CD31 (i), Runx1 (i,ii) and Kit (i,iii). Dotted lines demarcate the ventral (V, right) and dorsal (D, left) sides of the DA used for quantification of data in B. Scale bars: 100 µm. (B) Quantification of hematopoietic cluster cells ($CD31^+$ $Runx1^+$ Kit^+) in the dorsal and ventral aspects of the dorsal aortas of E10.5 embryos (mean±s.d.). One-way ANOVA and Tukey's, $^{**}P\leq0.01$, $^{*}P\leq0.05$. (C) Confocal *z*-projections of hearts in E10.5 embryos immunostained for CD31(i), Runx1 (i,ii) and Kit (i,iii). Arrows indicate ectopic angiogenic sprouts; arrowheads indicate ectopic $CD31^+Runx1^+Kit^+$ HSPCs in the atrium (A) and ventricle (V). Scale bars: 100 µm. (D) Quantification of the number of erythro-myeloid progenitors (EMPs) per heart (including atrium, ventricles and outflow tract) of E10.5 embryos (mean±s.d.). Data from 6 litters, one-way ANOVA and Tukey's multiple comparison test, $^{***}P\leq0.001$.

A potential reason for the loss of endothelial cell competency to respond to Runx1 after E7.5 is differences in the length of time Runx1 is ectopically expressed. Runx1 induction at E7.5 and analysis at E10.5 allows 72 h for HE cell specification and HSPC formation to occur, whereas induction at E9.5 allows only 24 h. To determine whether the length of time between induction and analysis was limiting, we induced Runx1 expression at E9.5 and analyzed the embryos at E12.5 (Fig. S4A). When we used 1 mg of tamoxifen to induce ectopic Runx1 expression at E9.5, the embryos died by E12.5 (not shown), so to prevent lethality we reduced the dose of tamoxifen to 0.5 mg. Despite the low dose of tamoxifen, Cre;cR1/+ embryos hemorrhaged and had flaky yolk sacs with poorly developed vasculature, but nevertheless survived (Fig. S4B). Flow analysis revealed no significant differences in the percentages of $CD144^+$ Kit^+ phenotypic HSPCs in either the embryo or yolk sac, but there were significantly fewer EMPs in Cre;cR1/+ embryos compared with littermate controls (Fig. S4C-E). These data indicate that the difference in the ability of E7.5 and E9.5 endothelial cells to produce HSPCs in response to Runx1 *in situ* reflects a difference in the competency of the endothelial cells to respond to Runx1 and/or in the permissiveness of the environment in which the endothelial cells are located for HSPC production.

Finally, we determined whether the increase in HSPCs induced by Runx1 was due to a higher frequency of HE cells. Ectopic Runx1 expression was initiated at E7.5 and endothelial cells purified from the embryo and yolk sac, and analyzed 24 h later (Fig. 4A). As HE cells are enriched in the Kit^+ population (Goldie et al., 2008; Marcelo et al., 2013; Nadin et al., 2003), we separated Kit^+ and Kit^- endothelial cells to determine whether Runx1 could specify Kit^- endothelial cells, which lack endogenous HE, to become hemogenic (Fig. 4B). We plated the endothelial cells on OP9 stromal cells in conditions demonstrated to support EHT (Swiers et al., 2013), and analyzed the wells 10 days later for the presence of $CD45^+$, $CD41^+$ and/or $Ter119^+$ hematopoietic cells. As expected, Kit^- endothelial cells from control cR1/+ yolk sacs and embryos contained no HE cells, whereas Kit^+ endothelial cells contained a low frequency of HE (Fig. 4C). The frequency of blood-producing HE cells in both the Kit^+ and Kit^- populations was significantly higher in Cre;cR1/+ embryos and yolk sacs compared with cR1/+ littermate controls. The ∼1:40 frequency of HE cells in Cre;cR1/+ embryos is particularly striking given that EMPs were not elevated in E10.5 embryos when Runx1 was induced at E7.5 (Fig. 3B). These data indicate that Runx1 alone can specify endothelial cells in the embryo proper as hemogenic. However, most endothelial cells in the embryo proper are located in a non-permissive environment that does not allow them to undergo an EHT and produce EMPs.

In conclusion, ectopic expression of Runx1 at E7.5 increases the number of EMPs in the yolk sac and heart *in vivo*, and can specify endothelial cells in both the yolk sac and embryo proper as hemogenic. The hemogenic potential of embryonic endothelial cells was revealed by their ability to differentiate into EMPs *in vitro*, as they could produce only a small increase in the number of HSPCs *in vivo*. Formation of the primitive vascular network occurs by E8 (Walls et al., 2008), and coincides with the formation of tight junctions between endothelial cells. Tight junctions have been shown to inhibit EHT (Yue et al., 2012; Zhang et al., 2014), and may explain why embryonic endothelial cells, which can be re-specified by Runx1 as hemogenic and can produce EMPs *ex vivo* following disaggregation, fail to do so *in vivo*. Other factors that may impair EMP formation in the embryo are the local absence of cytokines and/or the presence of inhibitory cell-cell interactions or signaling pathways. Finally, cell-intrinsic

Development (2018) 145, dev158162. doi:10.1242/dev.158162

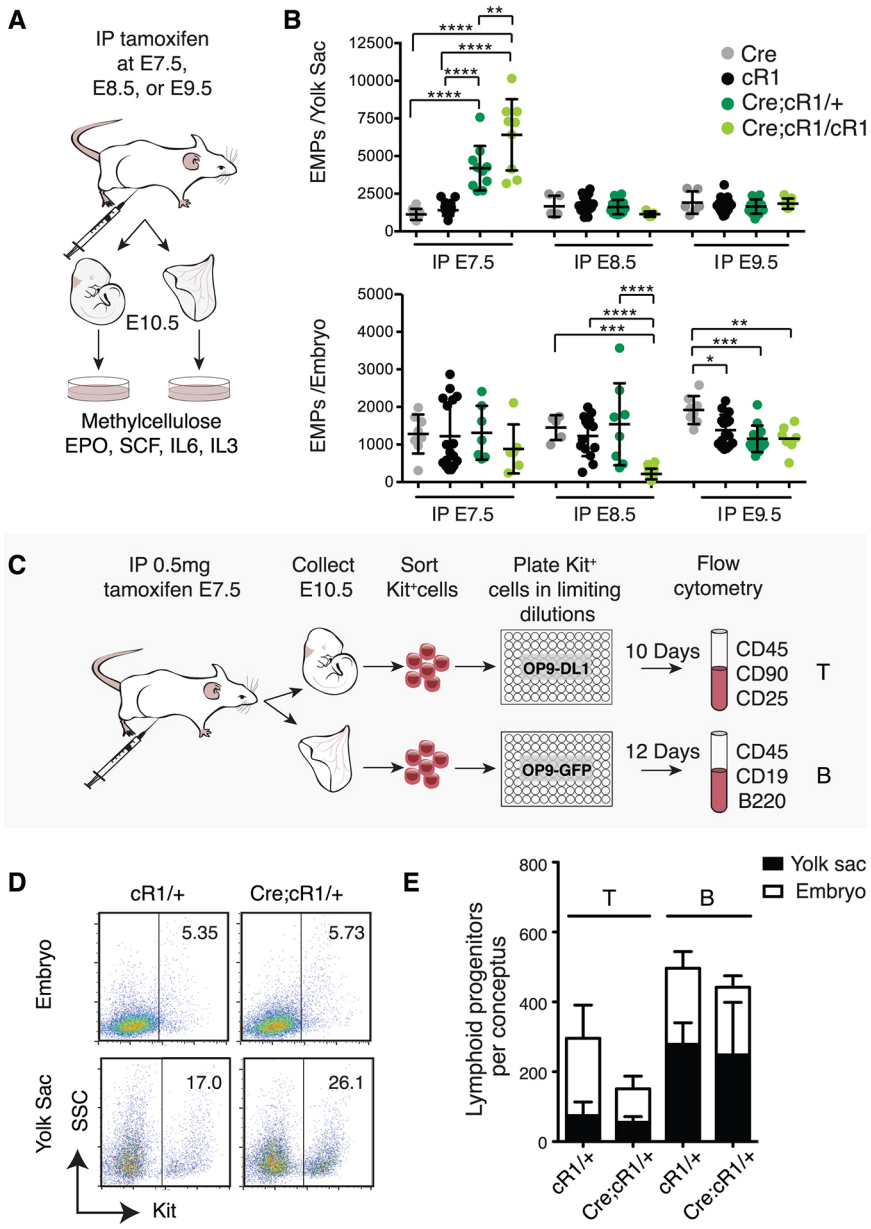

Fig. 3. Conditional endothelial-specific expression of Runx1 at E7.5, but not later, increases the total number of EMPs but not lymphoid progenitors. (A) Experimental outline for the quantification of EMPs in the yolk sac and embryo of E10.5 conceptuses after the initiation of ectopic Runx1 expression at E7.5, E8.5 or E9.5. (B) Total number of EMPs in the yolk sac and embryo of E10.5 conceptuses (mean±s.d.). Data are from 10, six and seven litters in which Runx1 was induced at E7.5, E8.5 and E9.5, respectively. One-way ANOVA and Tukey's multiple comparison tests, ****$P\leq0.0001$, ***$P\leq0.001$, **$P\leq0.01$, *$P\leq0.05$. (C) Experimental outline for the quantification of lymphoid progenitors. (D) Representative scatter plots of Kit$^+$ cells sorted for the limiting dilution analyses of lymphoid progenitors. (E) Total number of lymphoid progenitors within the Kit$^+$ population sorted from E10.5 embryos and yolk sacs after the initiation of Runx1 expression at E7.5 (mean±s.d.). Data from two independent experiments of pooled litters. Each dilution had 10 replicates per experiment. Unpaired two-tailed Student's *t*-test. B progenitors, $P\leq0.1482$; T progenitors, $P\leq0.6632$.

loss of competency may occur due to epigenetic changes that accompany the specialization of endothelial cells. Given the recent demonstration that hematopoietic stem cells can be generated by the introduction of four transcription factors (*FOSB*, *GFI1*, *RUNX1* and *SPI1*) into endothelial cells *in vitro* (Lis et al., 2017), understanding the barriers to HE specification and identifying endothelial cells most competent to respond to these transcription factors will be important for optimizing this reprogramming strategy for clinical applications.

MATERIALS AND METHODS

Mice

This study was performed in accordance with the recommendations in the Guide for the Care and Use of Laboratory Animals of the National Institutes of Health. All of the animals were handled according to the approved institutional animal care and use committee (IACUC) protocol #803789 of the University of Pennsylvania. We obtained Tg(Cdh5-cre/ERT2)1Rha mice (Sorensen et al., 2009) from Ralf Adams. Mice with a constitutively activated Runx1 cDNA in the *Rosa26* locus and *Runx1*$^{+/-}$ mice (*Runx1*^{tm1Spe}) have been described previously (Qi et al., 2017; Wang et al., 1996).

Superovulation

Three-week-old B6C3F1 females were injected intraperitoneally with 5 IU of gonadotropin from pregnant mare serum, and 48 h later with 5 IU of human chorionic gonadotropin (Sigma-Aldrich and the Los Angeles Biomedical Research Institute National Hormone & Peptide Program). Injected females were placed in cages with males at a 1:1 ratio for mating. Superovulated females were euthanized no later than E8.5.

Tamoxifen delivery

Tamoxifen free base (MP Biomedicals) was dissolved in ethanol then diluted in corn oil. Pregnant dams were injected intraperitoneally with 0.5-2.0 mg of tamoxifen.

Whole-mount immunofluorescence and confocal microscopy

Embryos were prepared as described previously (Yokomizo et al., 2012). The following primary antibodies were used: rat anti-mouse CD117 (Invitrogen, AB_467434, 1:250), rat anti-mouse CD31 (BD Pharmingen,

Development (2018) 145, dev158162. doi:10.1242/dev.158162

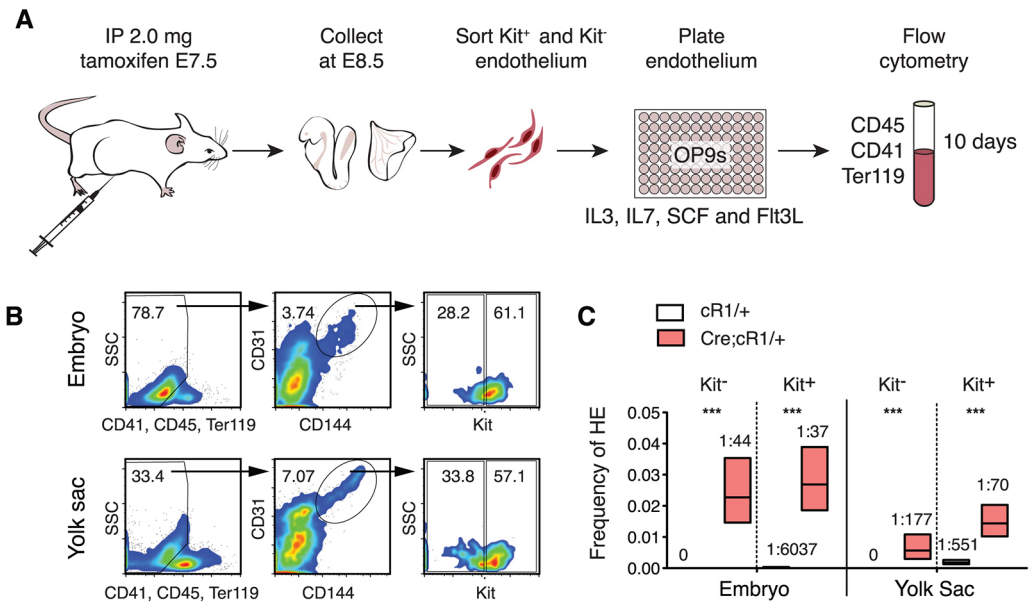

Fig. 4. Runx1 expression is sufficient to specify embryonic endothelial cells as hemogenic. (A) Illustration of a limiting dilution HE assay. (B) Representative scatter plot for isolation of Kit$^+$ and Kit$^-$ endothelial cells (CD41$^-$ CD45$^-$ Ter119$^-$ CD31$^+$ CD144$^+$) from E8.5 embryos and yolk sacs. (C) Frequency of HE cells in the Kit$^+$ and Kit$^-$ populations of CD41$^-$CD45$^-$Ter119$^-$CD31$^+$CD144$^+$ endothelial cells (±95% CI). Frequencies are indicated above the floating bars. Data represent four biological replicates for the cR1/+ Kit$^+$ yolk sac endothelial population and the cR1/+ Kit$^+$ embryonic endothelial population; three biological replicates for the Cre;cR1/+ Kit$^+$ yolk sac endothelial population, the cR1/+ Kit$^-$ yolk sac endothelial population, the Cre;cR1/+ Kit$^+$ embryonic endothelial population and the cR1/+ Kit$^-$ embryonic endothelial population; and two biological replicates for the Cre;cR1/+ Kit$^-$ yolk sac endothelial population and the Cre;cR1/+ Kit$^-$ embryonic endothelial population. Each replicate consisted of pooled cells from superovulated litters of E8.5 conceptuses collected in independent experiments. ***$P \leq 0.001$.

AB_394816, 1:500) and rabbit anti-human/mouse Runx (Abcam, AB_2049267, 1:250). Secondary antibodies were goat anti-rat Alexa Fluor 647 (Abcam, AB_141778, 1:1000), goat-anti rat Alexa Fluor 555 (Invitrogen, AB_141733, 1:1000) and goat anti-rabbit Alexa Fluor 488 (Life Technologies, AB_2576217, 1:1000). Images were acquired on a Zeiss LSM 710 AxioObserver inverted microscope with ZEN 2011 software. The Zeiss LSM 710 is equipped with 488, 543 and 633 nm wavelengths. Images were processed with Fiji software (Schindelin et al., 2012). Three-dimensional reconstructions were produced using Volocity software (Perkin Elmer).

Cell preparation

Embryonic cells were prepared for flow cytometry, cell sorting and progenitor assays as follows: embryos and yolk sacs were dissociated individually in 0.125% collagenase Type I (Sigma-Aldrich) for 20-30 min at 37°C. Fetal bovine serum (FBS, 20%) in PBS was added to samples to deactivate the collagenase, then the samples were triturated and filtered to obtain a single cell suspension.

Fluorescence-activated cell sorting and flow cytometry

The following antibodies were used: APC anti-CD144 (VEC) (eBioscience AB_10598508, 1:200), PE-Cy7 anti-CD31 (eBioscience, AB_469616, 1:200), APC anti-CD31 (BD Biosciences, AB_398497, 1:200), PerCP-eFluor710 anti-Kit (eBioscience, AB_1834421, 1:200), APC-eFluor780 anti-Kit (eBioscience, AB_1272177, 1:200), FITC anti-CD41 (Biolegend, AB_2129746, 1:400), PE anti-CD41 (BD Biosciences, AB_397004, 1:400), PerCP/Cy5.5 anti-CD45 (Biolegend, AB_893340, 1:500), FITC anti-CD45 (Biolegend, AB_312973, 1:500), FITC anti-Ter119 (Biolegend, AB_313707, 1:200), Alexa Fluor 700 anti-Ter119 (Biolegend, AB_528963, 1:200), PE-Cy7 anti-CD90 (eBioscience, AB_469642, 1:400), APC-Cy7 anti-CD25 (Biolegend, AB_830745, 1:400), APC anti-CD19 (eBioscience, AB_1659678, 1:400), PE-Cy7 anti-B220 (Bioscience, AB_469627, 1:400) and FITC anti-B220 (eBioscience, AB_465053, 1:400). DAPI was used to exclude dead cells. Cells were analyzed on an LSR II flow cytometer (BD Biosciences) and data were analyzed using FlowJo (Tree Star). Cells were sorted on a BD Influx with a 100 µm nozzle (BD Biosciences). For intracellular flow cytometry, the Foxp3/Transcription Factor Staining Buffer Set (eBiosciences) was used to fix and permeabilize cells. Fixable viability dye (eBioscience catalog# 65-0863-18, 1:1000) was used prior to fixing and permeabilizing cells to exclude dead cells. Rabbit anti-human/mouse Runx (Abcam, AB_2049267, 1:500) primary and goat anti-rabbit Alexa Fluor 647 (Life Technologies, AB_2535813, 1:500) secondary antibodies were used to immunostain embryonic cells for Runx1. All samples were treated with Fc block (AB_394657) prior to antibody staining.

Erythro-myeloid progenitor assay

Single cells were plated in MethoCult GF M3434 methylcellulose in duplicate (STEMCELL Technologies). Colonies were scored 7 days later.

Limiting dilution hemogenic endothelium assay

OP9 stromal cells were cultured in αMEM containing 10% FBS and antibiotics, and 1 day prior to the initiation of the HE assay were plated at a concentration of 4000 cells/well in 96-well plates. Sorted endothelial cells were plated in limiting dilutions with three to five replicates for each dilution on confluent OP9s. The media was supplemented with 10 ng/ml recombinant murine (rm) SCF, 10 ng/ml rm IL7, 10 ng/ml rm IL3 and 10 ng/ml rm Flt3L (all cytokines from PeproTech). On days 7-10, individual wells were inspected for hematopoietic cells via a phase contrast microscope; the cells were then harvested and analyzed by flow cytometry. Positive wells contained CD41$^+$, CD45$^+$ and/or Terr119$^+$ cells. The HE frequency was calculated using ELDA software (Hu and Smyth, 2009).

Lymphoid progenitor assay

Lymphoid assays were performed as previously described (Schmitt and Zúñiga-Pflücker, 2006). In brief, for limiting dilution assays, OP9 and OP9-DL1 stromal cells were plated in 96-well plates at a density of 4000 cells per well in αMEM containing 10% FBS and antibiotics. The next day, the medium was removed from the 96-well plates and B cell media containing αMEM, 10% FBS, antibiotics, 10 ng/ml rm IL7 and 5 ng/ml rm Flt3L was

added to the OP9 plates, and T cell media containing αMEM, 10% FBS, antibiotics, 1 ng/ml rm IL7 and 5 ng/ml rm Flt3L was added to the OP9-DL1 plates. Sorted Kit$^+$ cells were plated on the OP9s or OP9-DL1 cells in limiting dilutions. T cell cultures were analyzed 10 days after plating and B cell cultures 10-14 days after plating using flow cytometry. T cells were identified as CD45$^+$ CD25$^+$ CD90$^+$ and B cells as CD45$^+$ CD19$^+$ B220$^+$. The progenitor frequency was calculated using ELDA software (Hu and Smyth, 2009). OP9-MigR1 (OP9) and OP9-DL1 cells were kindly provided by W. S. Pear (University of Pennsylvania). Cell lines were confirmed to be mycoplasma free.

Acknowledgements
We thank Andrea Stout and Jasmine Zhao at the University of Pennsylvania Cell and Developmental Biology Microscopy Core for microscopy assistance, Qiufu Ma at Harvard Medical School for providing the Runx1 cR1 mice, and William DeMuth and Andrew Morschauser at the University of Pennsylvania Flow Cytometry and Cell Sorting Resource Laboratory for cell-sorting assistance.

Competing interests
The authors declare no competing or financial interests.

Author contributions
Conceptualization: A.D.Y., Y.L., N.A.S.; Methodology: A.D.Y., E.D.H., Y.L., N.A.S.; Software: A.D.Y., N.A.S.; Validation: A.D.Y., E.D.H., Z.L., N.A.S.; Formal analysis: A.D.Y., E.D.H., Y.L., N.A.S.; Investigation: A.D.Y., E.D.H., Y.L., Z.L., N.A.S.; Resources: A.D.Y., Y.L., Z.L., N.A.S.; Data curation: A.D.Y., E.D.H., N.A.S.; Writing - original draft: A.D.Y., N.A.S.; Writing - review & editing: A.D.Y., E.D.H., Y.L., Z.L., N.A.S.; Visualization: A.D.Y., N.A.S.; Supervision: N.A.S.; Project administration: N.A.S.; Funding acquisition: N.A.S.

Funding
This work was supported by the National Heart, Lung and Blood Institute (R01HL091724 and U01HL100405 to N.A.S.; 1F31HL120615 to A.D.Y.), the National Institute of Diabetes and Digestive and Kidney Diseases (T32 DK07780 to A.D.Y.), the National Cancer Institute (T32CA09140 to A.D.Y.), and the Leukemia and Lymphoma Society (Y.L). Deposited in PMC for release after 12 months.

Supplementary information
Supplementary information available online at
http://dev.biologists.org/lookup/doi/10.1242/dev.158162.supplemental

References
Chen, M. J., Yokomizo, T., Zeigler, B. M., Dzierzak, E. and Speck, N. A. (2009). Runx1 is required for the endothelial to haematopoietic cell transition but not thereafter. *Nature* **457**, 889-891.

Coultas, L., Chawengsaksophak, K. and Rossant, J. (2005). Endothelial cells and VEGF in vascular development. *Nature* **438**, 937-945.

Eliades, A., Wareing, S., Marinopoulou, E., Fadlullah, M. Z. H., Patel, R., Grabarek, J. B., Plusa, B., Lacaud, G. and Kouskoff, V. (2016). The hemogenic competence of endothelial progenitors is restricted by Runx1 silencing during embryonic development. *Cell Rep.* **15**, 2185-2199.

Frame, J. M., Fegan, K. H., Conway, S. J., McGrath, K. E. and Palis, J. (2015). Definitive hematopoiesis in the Yolk Sac emerges from Wnt-responsive hemogenic endothelium independently of circulation and arterial identity. *Stem Cells* **34**, 431-444.

Goldie, L. C., Lucitti, J. L., Dickinson, M. E. and Hirschi, K. K. (2008). Cell signaling directing the formation and function of hemogenic endothelium during murine embryogenesis. *Blood* **112**, 3194-3204.

Hu, Y. and Smyth, G. K. (2009). ELDA: extreme limiting dilution analysis for comparing depleted and enriched populations in stem cell and other assays. *J. Immunol. Methods* **347**, 70-78.

Huber, T. L., Kouskoff, V., Fehling, H. J., Palis, J. and Keller, G. (2004). Haemangioblast commitment is initiated in the primitive streak of the mouse embryo. *Nature* **432**, 625-630.

Lis, R., Karrasch, C. C., Poulos, M. G., Kunar, B., Redmond, D., Duran, J. G. B., Badwe, C. R., Schachterle, W., Ginsberg, M., Xiang, J. et al. (2017). Conversion of adult endothelium to immunocompetent haematopoietic stem cells. *Nature* **545**, 439-445.

Marcelo, K. L., Sills, T. M., Coskun, S., Vasavada, H., Sanglikar, S., Goldie, L. C. and Hirschi, K. K. (2013). Hemogenic endothelial cell specification requires c-Kit, Notch signaling, and p27-mediated cell-cycle control. *Dev. Cell* **27**, 504-515.

Nadin, B. M., Goodell, M. A. and Hirschi, K. K. (2003). Phenotype and hematopoietic potential of side population cells throughout embryonic development. *Blood* **102**, 2436-2443.

Nakano, H., Liu, X., Arshi, A., Nakashima, Y., van Handel, B., Sasidharan, R., Harmon, A. W., Shin, J.-H., Schwartz, R. J., Conway, S. J. et al. (2013). Haemogenic endocardium contributes to transient definitive haematopoiesis. *Nat. Commun.* **4**, 1564.

North, T. E., Gu, T.-L., Stacy, T., Wang, Q., Howard, L., Binder, M., Marín-Padilla, M. and Speck, N. A. (1999). *Cbfa2* is required for the formation of intra-aortic hematopoietic clusters. *Development* **126**, 2563-2575.

Qi, L., Huang, C., Wu, X., Tao, Y., Yan, J., Shi, T., Cao, C., Han, L., Qiu, M., Ma, Q. et al. (2017). Hierarchical Specification of Pruriceptors by Runt-Domain Transcription Factor Runx1. *J. Neurosci.* **37**, 5549-5561.

Rhodes, K. E., Gekas, C., Wang, Y., Lux, C. T., Francis, C. S., Chan, D. N., Conway, S., Orkin, S. H., Yoder, M. C. and Mikkola, H. K. (2008). The emergence of hematopoietic stem cells is initiated in the placental vasculature in the absence of circulation. *Cell Stem Cell* **2**, 252-263.

Sandler, V. M., Lis, R., Liu, Y., Kedem, A., James, D., Elemento, O., Butler, J. M., Scandura, J. M. and Rafii, S. (2014). Reprogramming human endothelial cells to haematopoietic cells requires vascular induction. *Nature* **511**, 312-318.

Schindelin, J., Arganda-Carreras, I., Frise, E., Kaynig, V., Longair, M., Pietzsch, T., Preibisch, S., Rueden, C., Saalfeld, S., Schmid, B. et al. (2012). Fiji: an open-source platform for biological-image analysis. *Nat. Methods* **9**, 676-682.

Schmitt, T. M. and Zúñiga-Pflücker, J. C. (2006). T-cell development, doing it in a dish. *Immunol. Rev.* **209**, 95-102.

Sorensen, I., Adams, R. H. and Gossler, A. (2009). DLL1-mediated Notch activation regulates endothelial identity in mouse fetal arteries. *Blood* **113**, 5680-5688.

Swiers, G., Baumann, C., O'Rourke, J., Giannoulatou, E., Taylor, S., Joshi, A., Moignard, V., Pina, C., Bee, T., Kokkaliaris, K. D. et al. (2013). Early dynamic fate changes in haemogenic endothelium characterized at the single-cell level. *Nat. Commun.* **4**, 2924.

Taoudi, S. and Medvinsky, A. (2007). Functional identification of the hematopoietic stem cell niche in the ventral domain of the embryonic dorsal aorta. *Proc. Natl. Acad. Sci. USA* **104**, 9399-9403.

Tober, J., Maijenburg, M. W. and Speck, N. A. (2016). Taking the leap: runx1 in the formation of blood from endothelium. *Curr. Top. Dev. Biol.* **118**, 113-162.

Walls, J. R., Coultas, L., Rossant, J. and Henkelman, R. M. (2008). Three-dimensional analysis of vascular development in the mouse embryo. *PLoS One* **3**, e2853.

Wang, Q., Stacy, T., Binder, M., Marín-Padilla, M., Sharpe, A. H. and Speck, N. A. (1996). Disruption of the *Cbfa2* gene causes necrosis and hemorrhaging in the central nervous system and blocks definitive hematopoiesis. *Proc. Natl. Acad. Sci. USA* **93**, 3444-3449.

Yokomizo, T. and Dzierzak, E. (2010). Three-dimensional cartography of hematopoietic clusters in the vasculature of whole mouse embryos. *Development* **137**, 3651-3661.

Yokomizo, T., Ogawa, M., Osato, M., Kanno, T., Yoshida, H., Fujimoto, T., Fraser, S., Nishikawa, S., Okada, H., Satake, M. et al. (2001). Requirement of Runx1/AML1/PEBP2aB for the generation of haematopoietic cells from endothelial cells. *Genes Cells* **6**, 13-23.

Yokomizo, T., Yamada-Inagawa, T., Yzaguirre, A. D., Chen, M. J., Speck, N. A. and Dzierzak, E. (2012). Whole-mount three-dimensional imaging of internally localized immunostained cells within mouse embryos. *Nat. Protoc.* **7**, 421-431.

Yue, R., Li, H., Liu, H., Li, Y., Wei, B., Gao, G., Jin, Y., Liu, T., Wei, L., Du, J. et al. (2012). Thrombin receptor regulates hematopoiesis and endothelial-to-hematopoietic transition. *Dev. Cell* **22**, 1092-1100.

Yzaguirre, A. D. and Speck, N. A. (2016). Insights into blood cell formation from hemogenic endothelium in lesser-known anatomic sites. *Dev. Dyn.* **245**, 1011-1028.

Zhang, C., Lv, J., He, Q., Wang, S., Gao, Y., Meng, A., Yang, X. and Liu, F. (2014). Inhibition of endothelial ERK signalling by Smad1/5 is essential for haematopoietic stem cell emergence. *Nat. Commun.* **5**, 3431.